

Lawrence Berkeley National Laboratory

Recent Work

Title

PHOTOEMISSION FROM Xe IN THE VICINITY OF THE 4d COOPER MINIMUM

Permalink

<https://escholarship.org/uc/item/17t3v38f>

Author

Lindle, D.W.

Publication Date

1987-09-01

e.2



Lawrence Berkeley Laboratory

UNIVERSITY OF CALIFORNIA

Materials & Chemical Sciences Division

RECEIVED
LAWRENCE
BERKELEY LABORATORY

JAN 8 1988

LIBRARY AND
DOCUMENTS SECTION

Submitted to Physical Review A

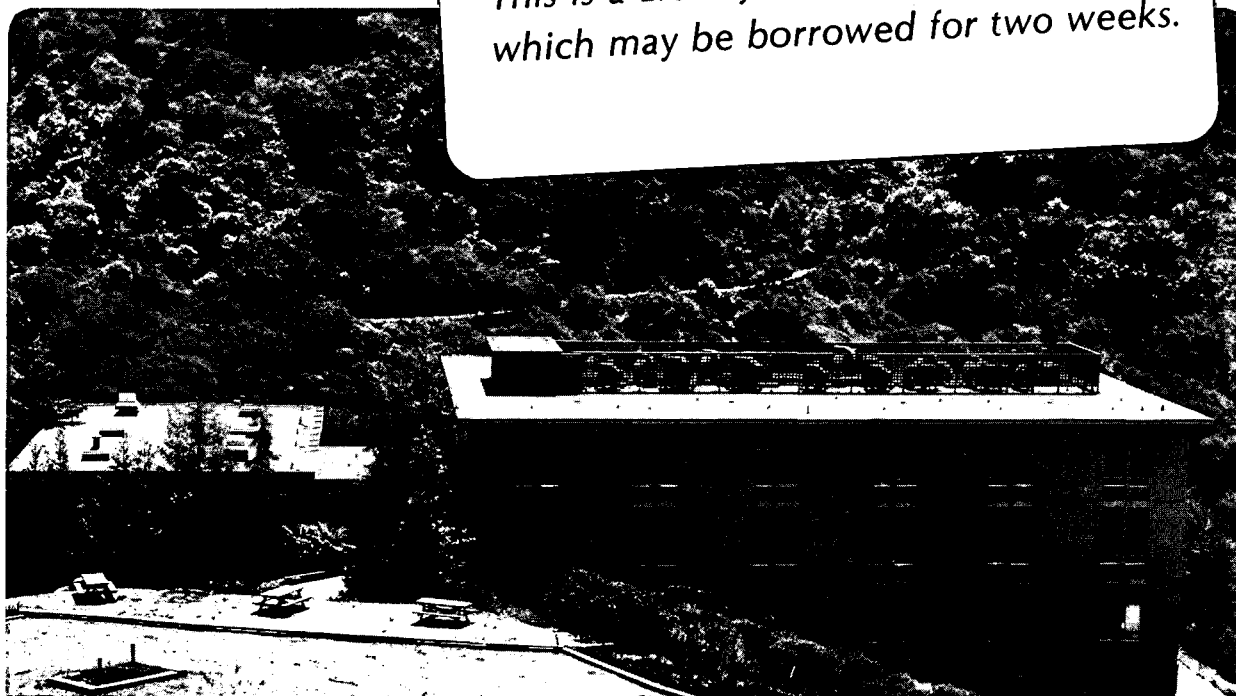
Photoemission from Xe in the Vicinity of the 4d Cooper Minimum

D.W. Lindle, T.A. Ferrett,
P.A. Heimann, and D.A. Shirley

September 1987

TWO-WEEK LOAN COPY

*This is a Library Circulating Copy
which may be borrowed for two weeks.*



LBL-22028
e.2

DISCLAIMER

This document was prepared as an account of work sponsored by the United States Government. While this document is believed to contain correct information, neither the United States Government nor any agency thereof, nor the Regents of the University of California, nor any of their employees, makes any warranty, express or implied, or assumes any legal responsibility for the accuracy, completeness, or usefulness of any information, apparatus, product, or process disclosed, or represents that its use would not infringe privately owned rights. Reference herein to any specific commercial product, process, or service by its trade name, trademark, manufacturer, or otherwise, does not necessarily constitute or imply its endorsement, recommendation, or favoring by the United States Government or any agency thereof, or the Regents of the University of California. The views and opinions of authors expressed herein do not necessarily state or reflect those of the United States Government or any agency thereof or the Regents of the University of California.

PHOTOEMISSION FROM Xe IN THE VICINITY OF THE 4d COOPER MINIMUM

D.W. Lindle, T.A. Ferrett, P.A. Heimann, and D.A. Shirley

Materials and Molecular Research Division
Lawrence Berkeley Laboratory
and
Department of Chemistry
University of California
Berkeley, California 94720

This work was supported by the Director, Office of Energy Research,
Office of Basic Energy Sciences, Materials Sciences Division of the
U.S. Department of Energy under Contract No. DE-AC03-76SF00098.

PHOTOEMISSION FROM Xe IN THE VICINITY OF THE 4d COOPER MINIMUM

D.W. Lindle,* T.A. Ferrett,* P.A. Heimann,[†] and D.A. Shirley

Materials and Molecular Research Division
Lawrence Berkeley Laboratory
and
Department of Chemistry
University of California
Berkeley, California 94720

Partial photoionization cross sections and angular-distribution asymmetry parameters have been determined for the Xe 4d and "4p" subshells in the photon-energy region of the 4d Cooper minimum (160 eV to 270 eV, to 520 eV for the 4d asymmetry parameter). The Cooper minimum is observed as a distinct cross-section minimum in the 4d photoionization channel. The 4d angular-distribution results are in excellent agreement with Dirac-Fock and relativistic random-phase approximation calculations and with previous measurements. Effects of interchannel coupling are evident in the "4p" results. Both the partial cross section and the angular distribution for the "4p" photoelectron peak track the 4d cross section and angular distribution as functions of photon energy. A similar result is observed for the summed intensity and the angular distribution of the 5p → np shake-up satellites of the 4d main line, which is probably due to the effects of electron correlation between the 4d and the satellite photoionization channels.

*Present address: National Bureau of Standards, Gaithersburg,
MD 20899.

[†]Present address: Technische Universität München, München, W. Germany.

I. Introduction

Inner-shell photoemission experiments on Xe have been used to study one-electron and multi-electron effects in atomic photoionization.¹⁻²² For example, photoemission from the Xe 4d subshell has shown that a series of single-electron processes combine to produce oscillations in both the subshell cross section^{5,6,10,11,15,16,19-22} and the angular-distribution asymmetry parameter^{4,8,14,15,21,22} over a wide range of photon energies beginning just above threshold. The lack of important many-electron effects on the 4d parameters can be attributed, in part, to the fact that the 4d photoemission channel dominates the absorption cross section for the Xe atom.^{5,11-13} By the same token, photoemission from other subshells in Xe, such as 5s and 5p, exhibit strong many-electron effects due to interchannel coupling with the 4d subshell.²⁰ For both of the valence subshells in Xe, changes in the partial cross section³ (and the asymmetry parameter for 5p^{7,9}) have been observed and identified as results of coupling to the stronger 4d channel.

At photon energies immediately above the 4d ionization threshold, the photoelectron spectrum is dominated by features associated with 4d-vacancy states. It is known^{8,15,20} that photoemission from the 4d subshell can be described accurately by the following series of one-electron effects that appear in the 4d \rightarrow ϵf continuum channel: a rapid change in the Coulomb phase occurs near threshold, followed at

somewhat higher energy by a centrifugal-barrier shape resonance,^{12,13,23} and finally at still higher energy, the $4d \rightarrow \epsilon f$ dipole matrix element experiences a change in sign which causes a "Cooper minimum" in the cross section.²⁴ Experimentally, pronounced changes have been observed in the absorption cross section,²⁵⁻²⁹ the $4d$ partial cross section,⁵ the spin-orbit branching ratio,⁶ and the angular distribution of Xe $4d$ photoelectrons.^{4,8} However, most of these earlier measurements, with one exception,⁸ have focussed on the energy region below the $4d$ Cooper minimum. The present work addresses the effects on $4d$ photoemission in the region of the Cooper minimum. The $4d$ partial cross section has been measured for the first time through the Cooper minimum. New results for the $4d$ asymmetry parameter also are presented. They improve significantly on our earlier measurements,⁸ and extend the angular-distribution results to higher energy (520 eV photon energy). Excellent agreement is observed with theoretical calculations^{15,21,22} of these primarily one-electron effects.

New results for the Xe " $4p$ " photoionization channel are presented here as well. They indicate that the " $4p$ " peak mimics the behavior of the $4d$ subshell throughout the photon-energy range of this work (185-270 eV). Single-electron calculations¹⁵ fail to predict this behavior, which is found to be quite similar to previous measurements³⁰ of isoelectronic I (in CH_3I). In the I " $4p$ " experiment, a tentative explanation was put forth in which the importance of the configuration $4d^8 4f$ to the ionic state reached by

"4p" ionization comes into play. It was suggested that one could regard the $4d^8 4f$ state as being a correlation satellite of the stronger 4d peak. In the present work, we discuss in addition the possibility of interchannel coupling between the 4d and "4p" channels, which can be viewed as being similar to the coupling between the 4d and the valence subshells (5s and 5p) of Xe. For the valence subshells, experimental observations^{3,7,9} illustrate that both peaks exhibit effects due to interchannel coupling in the photon-energy range of the 4d \rightarrow ϵf shape resonance (~ 100 eV).

A brief description of the experimental technique is given in Sec. II. The 4d and "4p" subshell results are presented in Sec. III, and conclusions are discussed in Sec. IV.

II. Experimental

The experiment was performed at the Stanford Synchrotron Radiation Laboratory with the same time-of-flight (TOF) apparatus³¹ and experimental conditions used in the previous work on CH_3I (Ref. 30) and Kr.³² For Xe, the monochromator resolution was a constant 1.3 Å at all photon energies.

For photoionization of a randomly oriented sample by linearly polarized radiation, Yang's theorem³³ defines the differential cross section in the dipole approximation as

$$\frac{d\sigma(h\nu, \theta)}{d\Omega} = \frac{\sigma(h\nu)}{4\pi} [1 + \beta(h\nu)P_2(\cos \theta)] \quad (1)$$

In Eq. (1), θ is the angle between the momentum vector of the ejected electron and the polarization vector of the ionizing radiation, $P_2(\cos \theta)$ is the second Legendre polynomial, and $\sigma(h\nu)$ and $\beta(h\nu)$ are the cross section and asymmetry parameter, respectively, for the photoionization process under study. Cross sections and asymmetry parameters are derived from photoelectron spectra taken with $\theta=0^\circ$ and $\theta=54.7^\circ$ as described in previous publications.^{30,32} At certain photon energies of the monochromator, second-order radiation (i.e. $2h\nu$) was sufficiently intense to produce peaks in our spectra, primarily second-order peaks from Xe 4d ionization. In this way, the 4d asymmetry-parameter results were extended to higher photon energy.

In the photon-energy range of the Xe experiment, it has been determined³⁴ that the scintillator sodium salicylate, which we use to measure the relative photon flux, has a monotonically increasing efficiency. Therefore, it was necessary to correct our relative cross-section measurements by as much as 50%. As a result, the usually quoted systematic errors of $\pm 10\%$ for our relative cross sections become $\pm 20\%$ in the high-energy region of the present measurements. The branching-ratio and asymmetry-parameter results, which are independent of the photon-flux measurement, have estimated systematic errors of $\pm 10\%$ and ± 0.1 , respectively. The estimated systematic errors are not included in the error bars of the data presented in this work.

III. Results and Discussion

A TOF photoelectron spectrum of Xe taken at 250 eV photon energy is shown in Fig. 1. This spectrum contains the unresolved $4d_{5/2}$ and $4d_{3/2}$ photoemission lines with binding energies of 67.5 eV and 69.5 eV, respectively. We also observe the "4p" peak (binding energy 145.5 eV¹) and an accompanying Coster-Kronig Auger feature near 50 eV kinetic energy. The enhanced intensity on the low-kinetic-energy side of the "4p" peak consists of many lines ($4d^8_{n\ell}$) and some continuum-like structure ($4d^8_{\epsilon\ell}$). A higher-resolution x-ray photoelectron spectrum of this kinetic-energy region can be found in Refs. 1 and 2. The remaining high-energy peaks result from photoionization of the valence subshells and from photoemission induced by higher-order components of the synchrotron radiation.

A. 4d Subshell

The 4d cross-section results are shown in the top portion of Fig. 2. All of the present cross-section measurements are given in arbitrary units, because of the lack of available quantitative information in the 160 to 270 eV photon-energy range. For example, we are unable to scale our relative peak intensities to the total absorption cross section²⁹ without further knowledge of the importance of direct multiple ionization. While there is evidence¹¹ that a considerable fraction of the total cross section above 100 eV

photon energy results from double ionization, there are no available quantitative measurements of this fraction. In addition, we were unable to determine quantitatively the relative intensity of the higher-binding-energy continuum-like structure to the left of the "4p" peak in Fig. 1. Finally, although there exist¹¹ 4d cross-section results on an absolute scale up to 160 eV, the overlap with the present work is insufficient to reliably scale our results. Thus, we report only relative cross sections.

The 4d cross-section data shown in the top of Fig. 2 exhibit a clear minimum which can be attributed to a Cooper minimum²⁴ in the 4d \rightarrow ϵ f photoemission channel. The rise to lower energies in Fig. 2 corresponds to the high-energy side of the prominent 4d \rightarrow ϵ f shape resonance^{12,13,23} that has been well-characterized in Xe. At higher photon energies, σ_{4d} recovers by more than a factor of two from its minimum value. The position of the Cooper minimum is 185(10) eV, in excellent agreement with absorption.²⁵⁻²⁹

The Xe 4d asymmetry-parameter results are shown in the bottom portion of Fig. 2, and over a wider photon-energy range in Fig. 3. Also included in these figures are previous measurements^{4,8} of β_{4d} and several theoretical curves.^{15,21,22} The experiments are in excellent agreement with each other and with the two relativistic calculations.^{21,22} The Dirac-Fock (DF)²¹ and relativistic random-phase approximation (RRPA)²² calculations predict the rapid decrease of β_{4d} at low energy, which is due to the Cooper minimum, and the asymptotic value of β_{4d} at higher energy. The

nonrelativistic Hartree-Fock (HF, velocity and length) calculations¹⁵ predict the correct shape of β_{4d} , but miss the energy of the Cooper minimum by 20-30 eV. The present results are in better agreement with theory at the minimum in β_{4d} . These new results are to be preferred over our earlier measurements⁸ in the regions of overlap, based on improved accuracy.

Using the expression for β in jj coupling,³⁵ β_{4d} is predicted to be approximately 0.2 at the Cooper minimum. This value for β_{4d} is reached at a photon energy between 175 and 180 eV, in fairly good, but not exact agreement with the 4d cross-section results.

At a few photon energies in the 160-182.5 eV range approaching the Cooper minimum, a 4d correlation satellite was resolved from the 4d photoemission main line (the satellite appears in Fig. 1 as a shoulder to the left of the 4d peak), allowing us to make a crude measurement of its intensity and angular distribution. This peak corresponds to the sum of the 5p \rightarrow np shake-up states.¹ Qualitatively, the intensity of this satellite peak relative to the 4d main line was found to be roughly constant throughout this energy range. Quantitatively, we measured the relative intensity to be 12(3)%, in disagreement with previous measurements of the satellite-to-main line ratio of 6(1)% at both 151 eV photon energy and at 1486 eV (Al $K\alpha$).³⁶ This discrepancy probably is explained by the poor kinetic-energy resolution of the present measurements, and by the presence of a background underlying the satellite peak which arises from Auger decay of the ionic states produced in the "4p"

binding-energy region. This background would not appear at either 151 eV or 1486 eV photon energy, because the satellite peak would be at a different kinetic energy than the underlying Auger electrons.

The asymmetry parameter for the sum of the $5p \rightarrow np$ satellites closely follows β_{4d} in this energy range, dropping from 1.4(2) at 160 eV to -0.6(2) at 182.5 eV. The present results indicate that the 4d correlation satellites seem to experience the Cooper minimum in the $4d \rightarrow \epsilon f$ channel at the same photon energy as the 4d main line. This is not expected in the conventional one-electron picture, in which the photoelectron's kinetic energy should determine the position of the Cooper minimum. However, in the presence of electron correlation, which clearly is important for a satellite lines, this result is not necessarily so unexpected. In fact, similar, but more dramatic, effects have been observed for a satellite in the 5 2p region of the molecule SF_6 .³⁷

B. "4p" Subshell

Gelius¹ and Svensson et al.² recorded Al $K\alpha$ photoelectron spectra of Xe in the region of the 4p binding energies. Rather than finding two peaks ($4p_{3/2}$ and $4p_{1/2}$) corresponding to one-electron transitions to Xe^+ , they found effects of multi-electron behavior in the photoelectron spectrum. Wendin and Ohno¹⁸ explained this phenomenon in Xe in terms of strong configuration mixing, which prevents the existence of an isolated $4p_{3/2}^-$ or $4p_{1/2}^-$ -hole state, and requires that a "4p" vacancy appear primarily as $Xe^+ (4d^8 4f)$.

The strong coupling results from the near degeneracy of a single 4p hole and a double vacancy with two 4d holes. A similar description is based on the onset of $N_{2,3}N_{4,5}N_{4,5}$ super-Coster-Kronig decay in the photon-energy range of "4p" ionization. The mixed-configuration identity of the "4p" line also is relevant to the "4p" Auger feature in Fig. 1. We can identify this peak as being related to either of the two processes, $Xe^+(4p^5) \rightarrow Xe^{++}(4d^9 5p^5)$ or $Xe^+(4d^8 4f) \rightarrow Xe^{++}(4d^9 5p^5)$, both of which yield Auger electrons of the appropriate energy.

The "4p" cross-section and asymmetry-parameter results for photon energies from 185 to 280 eV are shown in Fig. 4. These values were determined by considering only the area under the single prominent $(4d^8 4f)$ peak in Fig. 1 and excluding insofar as possible the continuum-like structure at lower kinetic energy. We will interpret the data in Fig. 4 as primarily representing the $4d^8 4f$ final state.

The Xe "4p" cross-section data in the top portion of Fig. 4 are on the same arbitrary scale as σ_{4d} in Fig. 2. The intensity of the $4d^8 4f$ peak accounts for less than half of the total intensity in the "4p" region, the remainder being in the broad continuum structure seen in Fig. 1. Thus, the cross section for all of the photoemission occurring in the "4p" binding-energy region is of the same order as σ_{4d} in the vicinity of the 4d Cooper minimum. Also in the top of Fig. 4 is a curve which represents a smooth function through the σ_{4d} results in the top of Fig. 2, divided by four. From this comparison, we observe that the cross section of the "4p" peak varies with σ_{4d} , and possibly experiences the Cooper minimum in the $4d \rightarrow \epsilon f$ channel.

The "4p" asymmetry-parameter results in the bottom portion of Fig. 4 also exhibit behavior very similar to β_{4d} , which is represented by the solid curve in the bottom panel. Also included in this panel is a curve representing a HF-V calculation,¹⁵ which predicts β_{4p} within a one-electron approximation. Clearly, the curve representing β_{4d} matches the "4p" results better than the HF-V curve. An identical observation has been made for $\beta_{"4p"}$ and β_{4d} for the I atom in CH_3I .³⁰

The similarities between the measured parameters for the Xe "4p" and 4d subshells are striking. In the work on CH_3I ,³⁰ recourse was made to the identification of the "4p" peak with the $4d^8 4f$ configuration in order to liken the "4p" peak to a correlation satellite of the $4d^9$ main-line final state. Therefore, the "4p" peak may be considered to be derived from the 4d main line, and thus might be expected to mimic the 4d behavior as a function of energy. However, there are two problems with this picture. First, the binding-energy difference between the $4d^8 4f$ and $4d^9$ ionic states is large (~ 70 eV), suggesting that the large difference in kinetic energies of the 4d and "4p" photoelectrons may lead to different cross sections and angular distributions as a function of photon energy (kinetic-energy effect). Second, the $4d^8 4f$ state designated as a satellite would correspond heuristically to a $4d \rightarrow 4f$ excitation accompanying 4d ionization, which is similar to a "conjugate shake-up" satellite, from which behavior different than the main line may be expected.³⁸

While the description of the "4p" peak as a satellite of the 4d line is possible, there is a different picture within which to discuss the observed similarities for the 4d and "4p" data. It is known that interchannel coupling with the 4d continuum plays an important role for the Xe valence shell. At photon energies near the 4d \rightarrow ϵf shape resonance, the 5s and 5p subshells exhibit enhancement³ which has been attributed to coupling with the 4d channel.²⁰ Similarly, if the 4d channel were to couple with the "4p" subshell, one might expect the "4p" cross section and asymmetry parameter to exhibit effects of this coupling. The exact mechanism by which the 4d and the 4d⁸4f photoemission channels could couple through the continuum and lead to the same spectral shape for their cross sections and asymmetry parameters requires further theoretical understanding. In addition, the extent to which the 4d⁸4f configuration, identified with the "4p" peak, plays the role of a satellite of the 4d line is unknown, and needs to be determined with a dynamical calculation that properly treats the many-electron nature of the "4p" region of the Xe spectrum.

IV. Conclusions

Inner-shell photoemission from Xe in the vicinity of the 4d Cooper minimum has been reported. The new results for σ_{4d} and β_{4d} illustrate dramatic effects due to the zero in the 4d \rightarrow ϵf transition amplitude. We observe excellent agreement with previous measurements and with relativistic calculations which treat 4d ionization in a single-electron framework.

In contrast, many-electron effects appear to be important for describing photoionization of both the "4p" subshell and the $5p \rightarrow np$ shake-up satellites of the 4d main line. The results for each of these photoemission channels resemble σ_{4d} and β_{4d} throughout the energy range of the 4d Cooper minimum, suggesting the possibility of strong interchannel coupling and main line-satellite interactions, or possibly a combination of both effects for "4p" ionization. This general picture of the importance of many-electron effects tied to the 4d subshell seems to be valid even though the 4d channel is experiencing a minimum in this energy range, and thus does not dominate the photoionization process. Further theoretical work is needed to clarify the coupling by which the 4d photoemission process exerts such an influence over the other Xe photoionization channels in this energy range.

Acknowledgements

The authors wish to thank S.T. Manson for helpful discussions. This work was supported by the Director, Office of Energy Research, Office of Basic Energy Sciences, Chemical Sciences Division of the U.S. Department of Energy under Contract No. DE-AC03-76SF00098. It was performed at the Stanford Synchrotron Radiation Laboratory, which is supported by the Department of Energy's Office of Basic Energy Sciences.

References

1. U. Gelius, J. Electron Spectrosc. 5, 985 (1974).
2. S. Svensson, N. Mårtensson, E. Basilier, P.Å. Malmquist, U. Gelius, and K. Siegbahn, Phys. Scr. 14, 141 (1976).
3. J.B. West, P.R. Woodruff, K. Codling, and R.G. Houlgate, J. Phys. B 9, 407 (1976).
4. L. Torop, J. Morton, and J.B. West, J. Phys. B 9, 2035 (1976).
5. S.P. Shannon, K. Codling, and J.B. West J. Phys. B 10, 825 (1977).
6. M.S. Banna, M.O. Krause, and F. Wuilleumier, J. Phys. B 12, L125 (1979).
7. M.O. Krause, T.A. Carlson, and P.R. Woodruff, Phys. Rev. A 24, 1374 (1981).
8. S.H. Southworth, P.H. Kobrin, C.M. Truesdale, D. Lindle, S. Owaki, and D.A. Shirley, Phys. Rev. A 24, 2257 (1981).
9. S. Southworth, U. Becker, C.M. Truesdale, P.H. Kobrin, D.W. Lindle, S. Owaki, and D.A. Shirley, Phys. Rev. A 28, 261 (1983).
10. B.W. Yates, K.H. Tan, L.L. Coatsworth, and G.M. Bancroft, Phys. Rev. A 31, 1529 (1985).
11. U. Becker, T. Prescher, E. Schmidt, B. Sonntag, and H.-E. Wetzel, Phys. Rev. A 33, 3891 (1986).
12. J.W. Cooper, Phys. Rev. Lett. 13, 762 (1964).
13. S.T. Manson and D.J. Kennedy, Chem. Phys. Lett. 7, 387 (1970).
14. S.T. Manson, Phys. Rev. Lett. 26, 219 (1971).
15. D.J. Kennedy and S.T. Manson, Phys. Rev. A 5, 227 (1972).

16. M.Y. Amusia, N.B. Berezina, and L.V. Chernysheva, Phys. Lett. 51A, 101 (1975).
17. M.Y. Amusia and V.K. Ivanov, Phys. Lett. 59A, 194 (1976).
18. G. Wendin and M. Ohno, Phys. Scr. 14, 148 (1976).
19. W.R. Johnson and V. Radojević, J. Phys. B 11, L773 (1978).
20. M.Y. Amusia, Comments At. Mol. Phys. 8, 61 (1979).
21. W. Ong and S.T. Manson (unpublished results).
22. K.-N. Huang, W.R. Johnson, and K.T. Cheng, At. Data Nucl. Data Tables 26, 33 (1981) and unpublished results.
23. S.T. Manson and J.W. Cooper, Phys. Rev. 165, 126 (1968).
24. J.W. Cooper, Phys. Rev. 128, 681 (1962).
25. A.P. Lukirskii, I.A. Brytov, and T.M. Zimkina, Opt. Spektrosk. 17, 438 (1964) [Opt. Spectrosc. 17, 234 (1964)].
26. D.L. Ederer, Phys. Rev. Lett. 13, 760 (1964).
27. T.M. Zimkina and S.A. Gribovskii, J. Phys. (Paris) Colloq. 10, C4-282 (1971).
28. J.P. Connerade, Proc. R. Soc. London, Ser. A 347, 581 (1976).
29. J.B. West and J. Morton, At. Data Nucl. Data Tables 22, 103 (1978).
30. D.W. Lindle, P.H. Kobrin, C.M. Truesdale, T.A. Ferrett, P.A. Heimann, H.G. Kerkhoff, U. Becker, and D.A. Shirley, Phys. Rev. A 30, 239 (1984).
31. M.G. White, R.A. Rosenberg, G. Gabor, E.D. Poliakoff, G. Thornton, S. Southworth, and D.A. Shirley, Rev. Sci. Instrum. 50, 1288 (1979).

32. D.W. Lindle, P.A. Heimann, T.A. Ferrett, P.H. Kobrin, C.M. Truesdale, U. Becker, H.G. Kerkhoff, and D.A. Shirley, Phys. Rev. A 33, 319 (1986).
33. C.N. Yang, Phys. Rev. 74, 764 (1948).
34. D.W. Lindle, T.A. Ferrett, P.A. Heimann, and D.A. Shirley, Phys. Rev. A 34, 1131 (1986); G.C. Angle, J.A.R. Samson and G. Williams, Appl. Optics 25, 3312 (1986); J. Nordgren and R. Nyholm (private communication).
35. T.E.H. Walker and J.T. Waber, J. Phys. B 6, 1165 (1973).
36. D.P. Spears, H.J. Fischbeck, and T.A. Carlson, Phys. Rev. A 9, 1603 (1974).
37. T.A. Ferrett, D.W. Lindle, P.A. Heimann, M.N. Piancastelli, P.H. Kobrin, H.B. Kerkhoff, U. Becker, W.D. Brewer, and D. A. Shirley (unpublished results).
38. For example, $\text{He}^+(2p)$, as in D.W. Lindle, T.A. Ferrett, U. Becker, P.H. Kobrin, C.M. Truesdale, H.G. Kerkhoff, and D.A. Shirley, Phys. Rev. A 31, 714 (1985) and references therein.

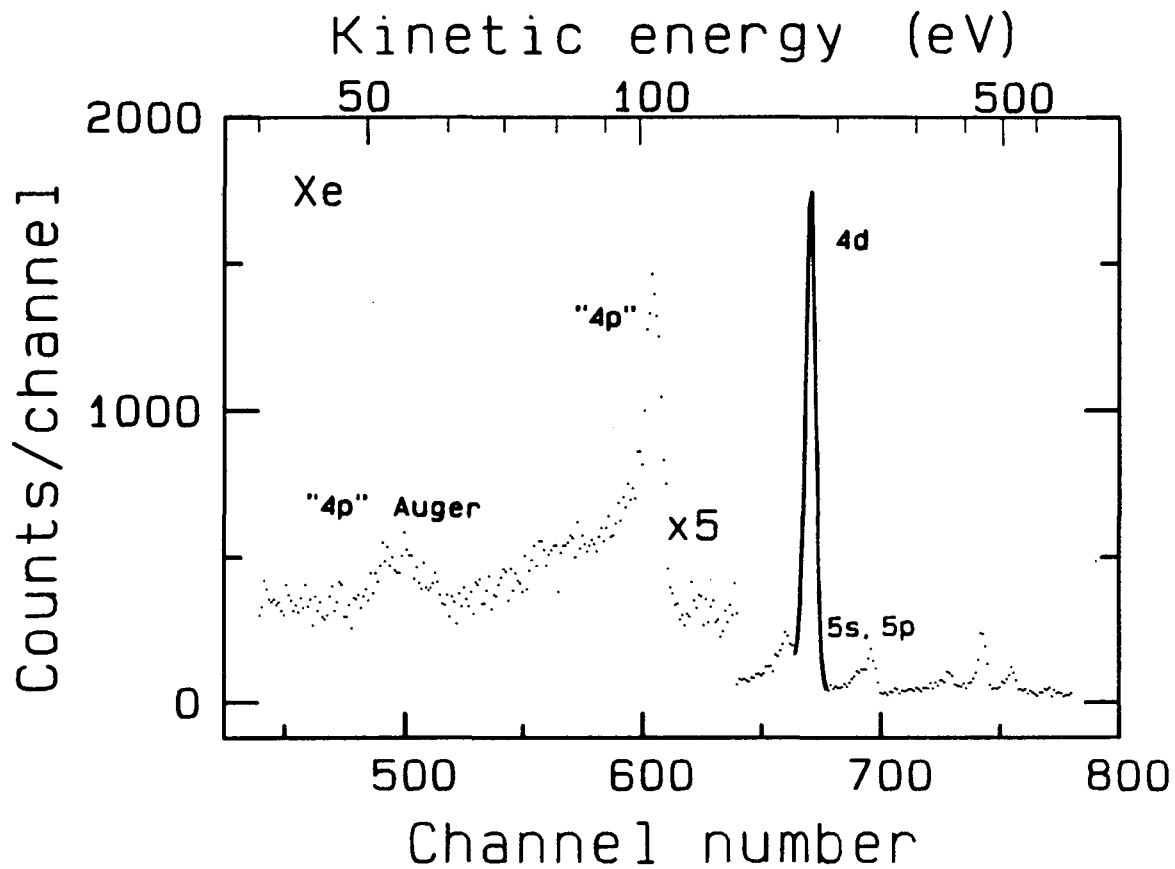
Figure Captions

Fig. 1 TOF photoelectron spectrum of Xe at 250 eV photon energy and with $\theta=54.7^\circ$. The peaks at high kinetic energy result from photoionization by higher-order components of the synchrotron radiation.

Fig. 2 Partial cross section (top) and asymmetry parameter (bottom) of the Xe 4d subshell. The experimental measurements are from the present work (closed) and from Ref. 8 (open). The theoretical curves in the bottom panel are from Refs. 21 (DF), 22 (RRPA), and 15 (HF-V, HF-L).

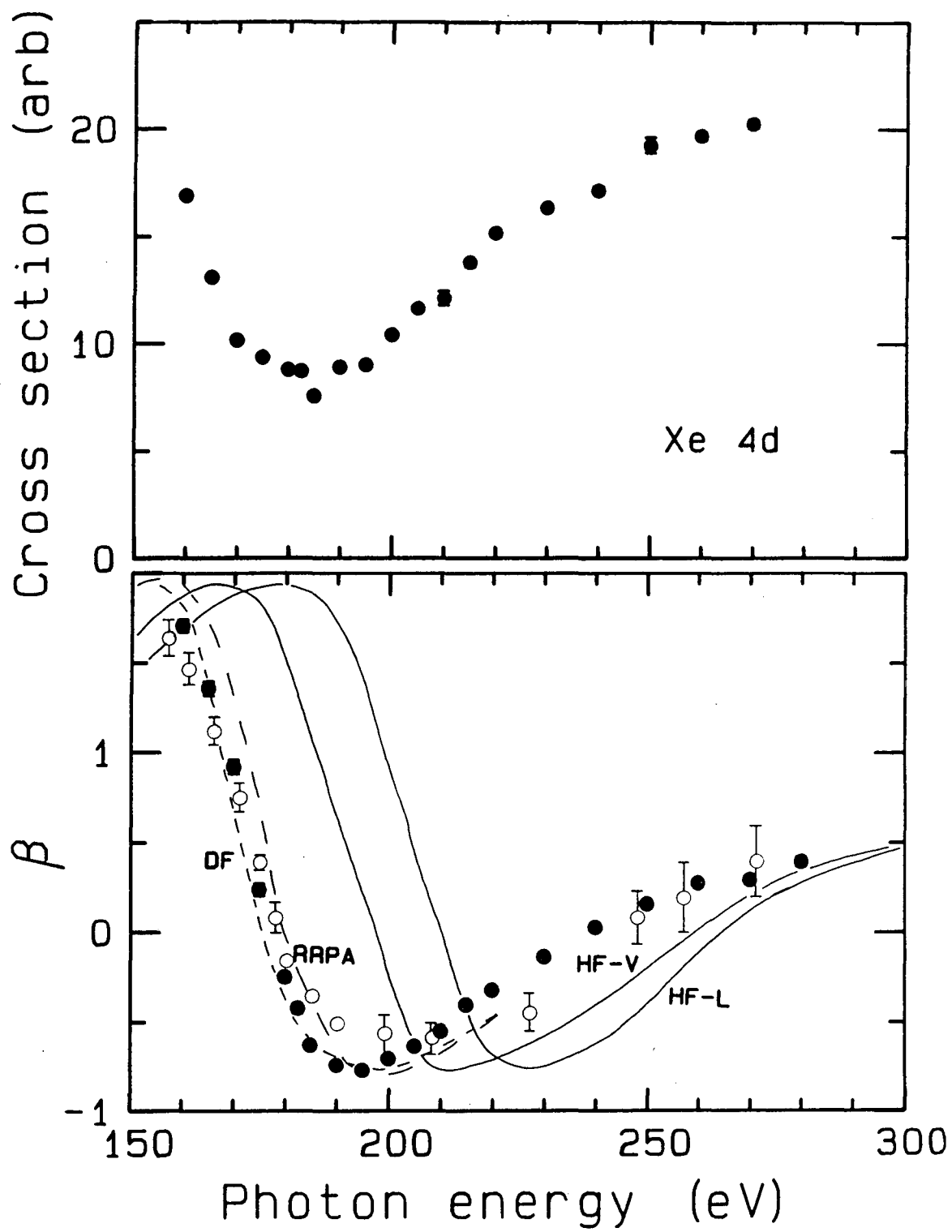
Fig. 3 Asymmetry parameter of the Xe 4d subshell as in the bottom panel of Fig. 2, now including experimental results from Ref. 4 (X), plotted over a wider photon-energy range.

Fig. 4 Partial cross section (top) and asymmetry parameter (bottom) of the Xe "4p" ($4d^8 4f$) photoelectron peak. The cross section is on the same arbitrary scale as σ_{4d} in the top panel of Fig. 2. The solid curves represent the σ_{4d} (divided by 4) and β_{4d} data in Fig. 2, and the dashed curve represents a HF-V calculation of β_{4p} (Ref. 15).



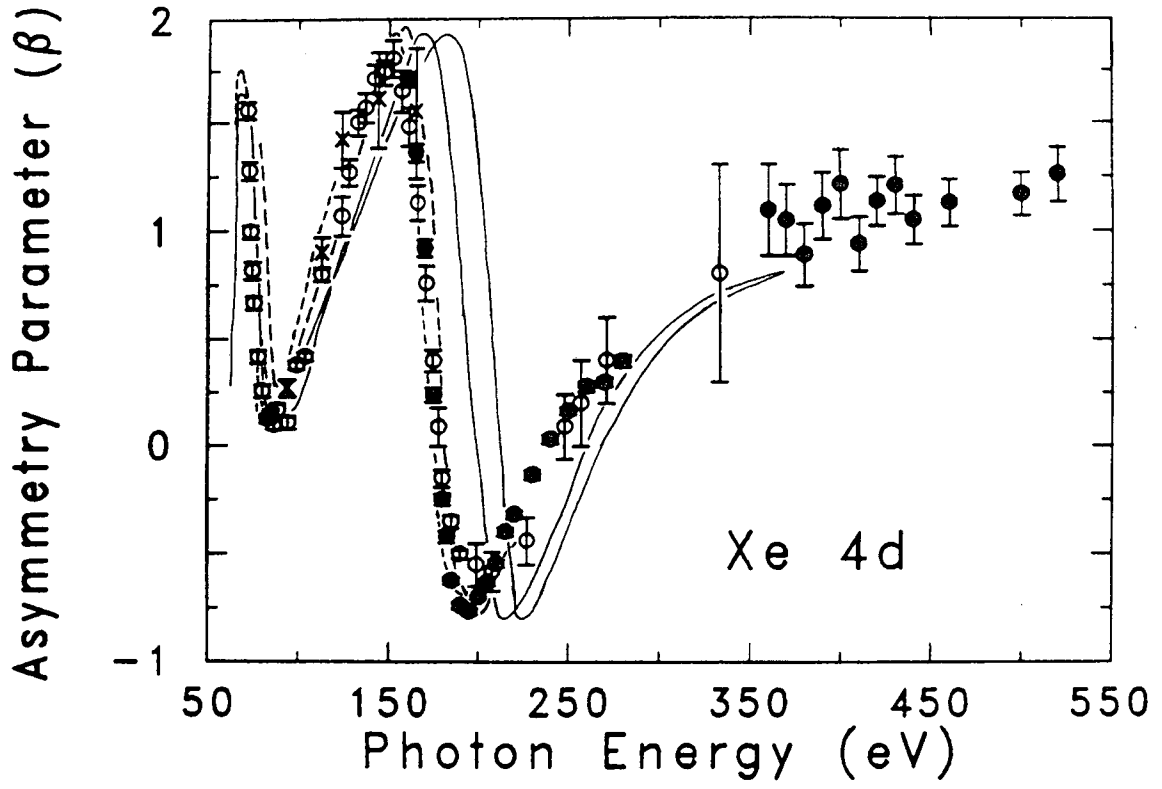
XBL 877-3355

Figure 1



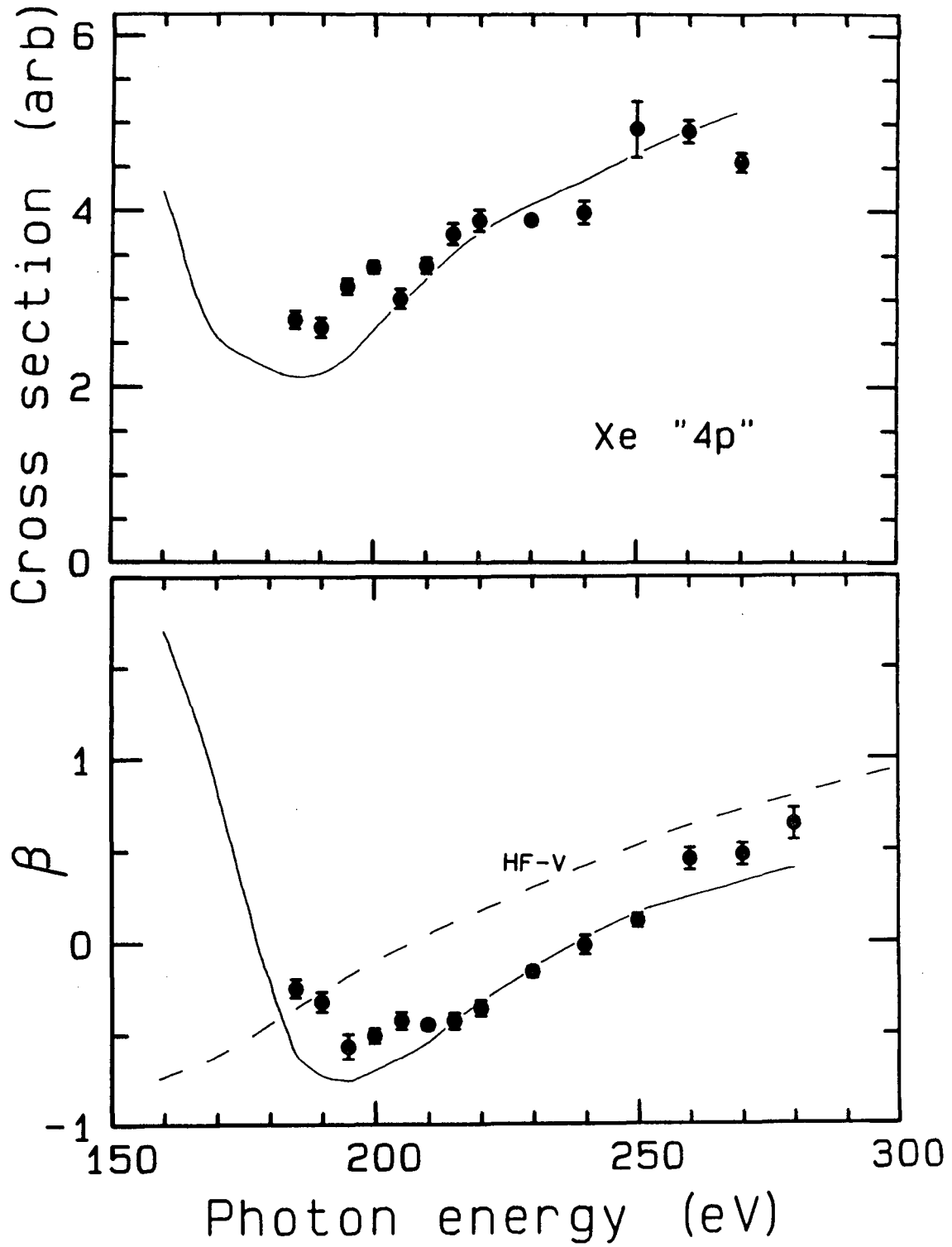
XBL 877-3354

Figure 2



XBL 8710-4407

Figure 3



XBL 877-3352

Figure 4

*LAWRENCE BERKELEY LABORATORY
TECHNICAL INFORMATION DEPARTMENT
UNIVERSITY OF CALIFORNIA
BERKELEY, CALIFORNIA 94720*